Goddard Space Flight Center

# Planetary Crater Detection and Registration Using Marked Point Processes, Multiple Birth and Death Algorithms, and Region-based Analysis

David Solarna[2], Gabriele Moser[2],
Jacqueline Le Moigne[1], and Sebastiano B. Serpico[2]

[1] NASA Goddard Space Flight Center
[2] University of Genoa

IGARSS 2017, Fort Worth, Texas, July 2017

# Content

**Introduction**

**Crater Detection**

- Marked Point Process Model
- Energy Function
- Multiple Birth and Death Algorithm
- Region-of-Interest Approach
- Experimental Results

**Image Registration**

- 2-step Approach
- Experimental Results

**Conclusion**

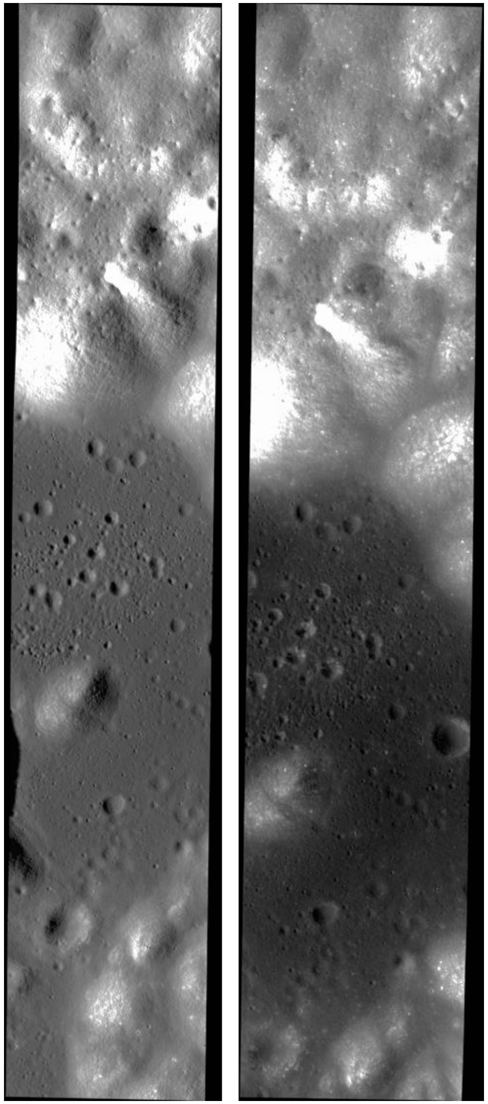

# Content

## Introduction

## Crater Detection

- Marked Point Process Model
- Energy Function
- Multiple Birth and Death Algorithm
- Region-of-Interest Approach
- Experimental Results

## Image Registration

- 2-step Approach
- Experimental Results

## Conclusion

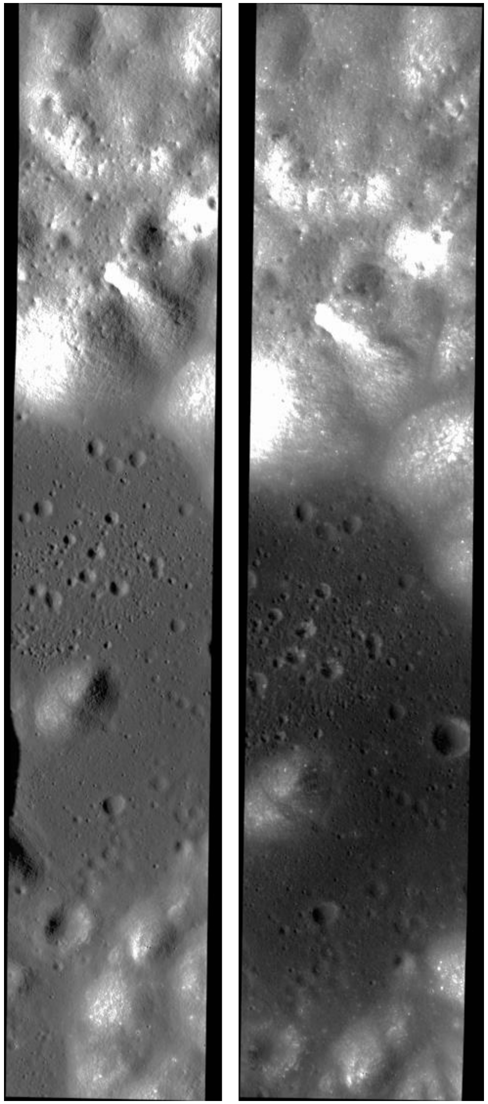

# Introduction

## Need for automated methods for image registration

Launch of several planetary missions

Design of new and powerful sensors

Large data sets

Multisensor

Multitemporal

Both

## Objective

- **Crater detection** in planetary images
- Development of an **image registration** method based on the **extracted features**

Original Data Set

Crater Detection → Crater Map

Crater Detection → Crater Map

Registration

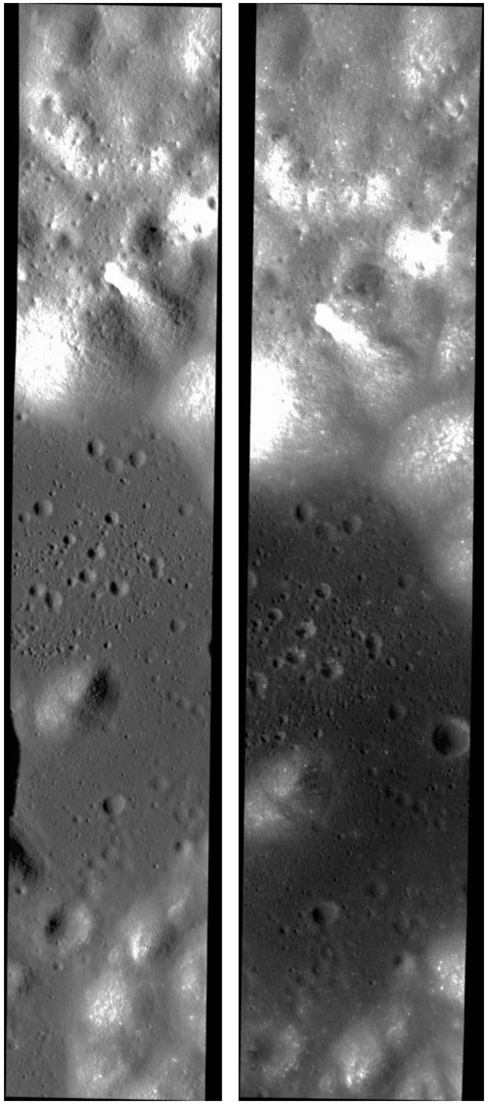

# Content

**Introduction**

**Crater Detection**

- Marked Point Process Model
- Energy Function
- Multiple Birth and Death Algorithm
- Region-of-Interest Approach
- Experimental Results

**Image Registration**

- 2-step Approach
- Experimental Results

**Conclusion**

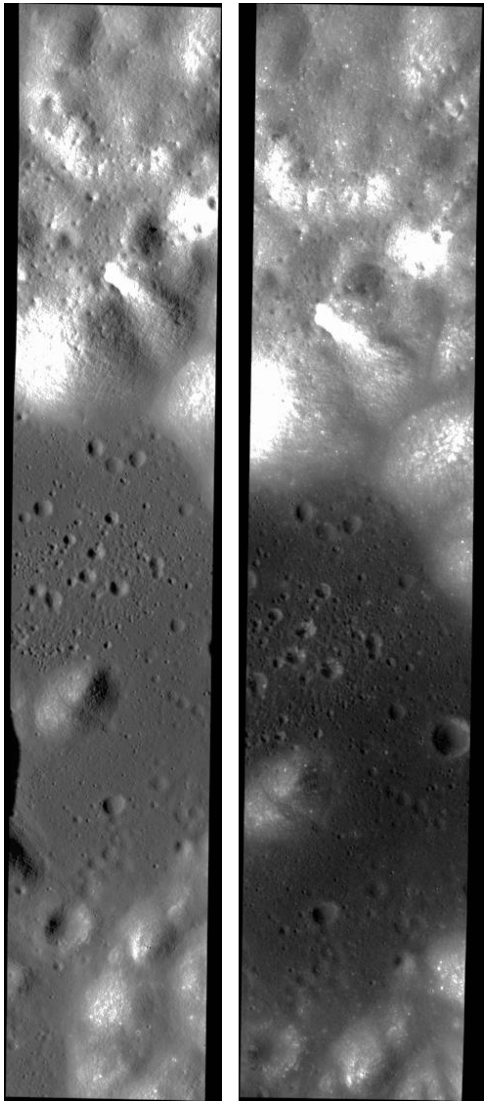

# Marked Point Processes

## Crater detection based on a marked point process (MPP) model

MPP: Stochastic Process $\xrightarrow{\text{Realizations}}$ Configurations of objects, each described by a marked point

### Mathematical Formulation

A **point process** $X$, defined over a bounded subset $P$ of $\mathbb{R}^2$ maps from a probability space to a **configuration of points** in $P$.

**Realizations** of the process $X$ are **random configurations** $x$ **of points**, $x = \{\boldsymbol{x}_1, \ldots, \boldsymbol{x}_n\}$, where $\boldsymbol{x}_i$ is the **location** of the $i^{\text{th}}$ point in the **image plane** ($\boldsymbol{x}_i \in P$)

A **configuration** of an **MPP** consists of a point process whose **points are enriched with additional parameters**, called **marks** and aimed at parameterizing objects linked to the points.

**Bayesian approach**: Maximum *a posteriori* (MAP) rule to **fit the model** to the image is equivalent to **minimizing an energy function** (computationally challenging)

# Marked Point Process for Crater Detection

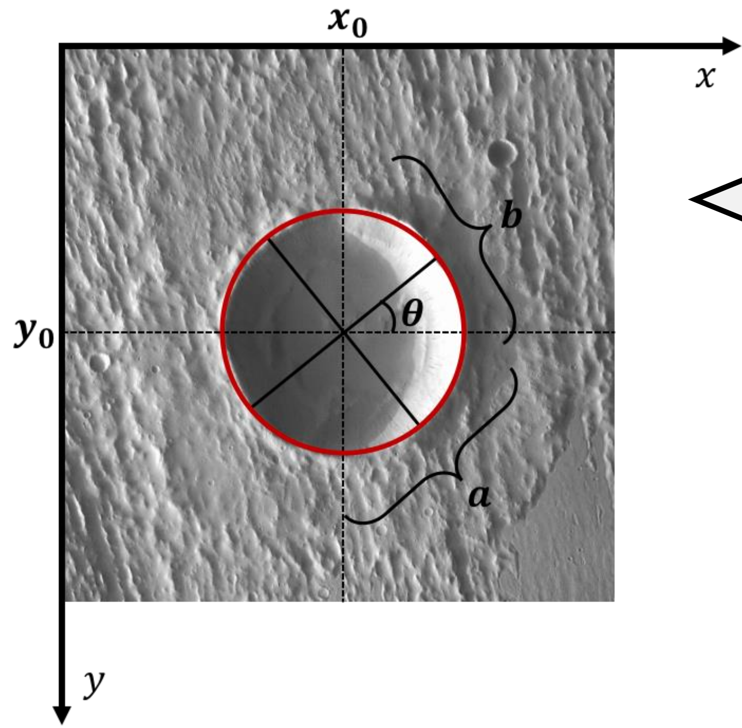


## Modelling

Crater → Ellipse

Distribution of craters on the surface → Distribution of ellipses on the image plane

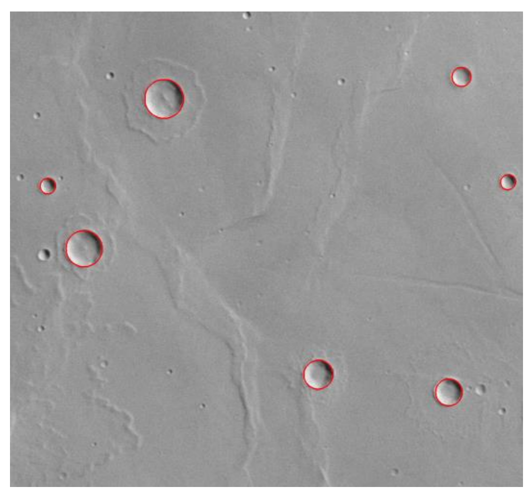

Realization Example

*Point Process*

$$x = \{\boldsymbol{x}_1, \dots, \boldsymbol{x}_7\}$$

*Parameters*

$$\boldsymbol{x}_i = (x_{0i}, y_{0i}, a_i, b_i, \theta_i)$$

**Craters**

- Center: $(x_0, y_0)$ } Point
- Major Axis: $a$
- Minor Axis: $b$
- Orientation: $\theta$

} Marks

# Crater Detection – Energy Function

**Energy function** of the configuration $X = \{\boldsymbol{x}_i, \boldsymbol{x}_2, \dots, \boldsymbol{x}_n\}$ wrt the extracted set $C$ of **contour pixels** (Canny):

$$U(X|C) = U_P(X) + U_L(C|X)$$

## Prior

**Repulsion** coefficient based on the overlapping of the ellipses (overlapping craters are quite unlikely)

$$U_P(X) = \frac{1}{n} \sum_{\boldsymbol{x}_i \wedge \boldsymbol{x}_j > 0} \frac{\boldsymbol{x}_i \wedge \boldsymbol{x}_j}{\boldsymbol{x}_i \vee \boldsymbol{x}_j}$$

$\boldsymbol{x}_i \vee \boldsymbol{x}_j$= area of union of ellipses $\boldsymbol{x}_i$ and $\boldsymbol{x}_j$

$\boldsymbol{x}_i \wedge \boldsymbol{x}_j$= area of intersection of $\boldsymbol{x}_i$ and $\boldsymbol{x}_j$

## Likelihood

Two terms, one based on a **correlation** measure, the other based on a **distance** measure (fit between contours and realization of $X$)

$$U_L(C|X) = \sum_{i=1}^{n} \left[ \frac{d_{\mathcal{H}}(x_i^0, C)}{n a_i} - \frac{|x_i^0 \cap C|}{|C|} \right]$$

$x_i^0$ = set of pixels corresponding to ellipse $\boldsymbol{x}_i$ in the image plane

$d_{\mathcal{H}}(x_i^0, C)$ = Hausdorff distance between ellipse $\boldsymbol{x}_i$ and the contours:

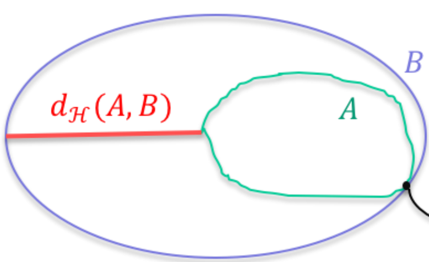


$$d_{\mathcal{H}}(A, B) = \max\left\{ \sup_{\alpha \in A} \inf_{\beta \in B} d(\alpha, \beta) \, ; \, \sup_{\beta \in B} \inf_{\alpha \in A} d(\alpha, \beta) \right\}$$

Classical distance between sets $d(A, B) = 0$

# Crater Detection – Energy Minimization

Markov chain Monte Carlo-type method
Simulated Annealing scheme

Markov chain sampled by a multiple birth and death (MBD) algorithm

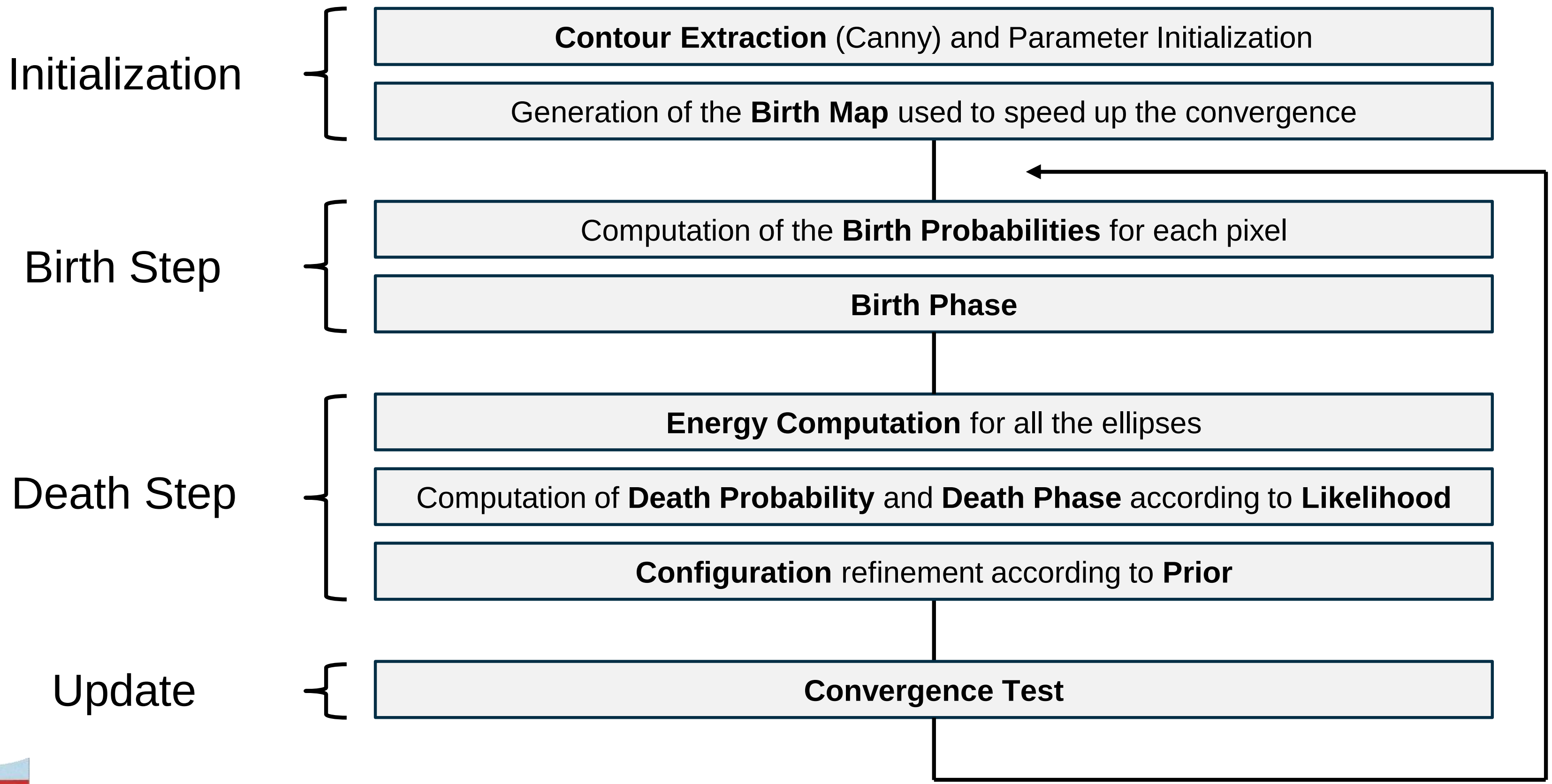

# MBD – Birth and Death Steps

## Birth Step

For **each pixel** $s$ in the image, compute the **birth probability** as $\min\{\delta \cdot B(s), 1\}$, where:

$$B(s) = \frac{b(s)}{\sum_s b(s)}$$

$b(s)$ is the **birth map** computed from the contour map using generalized Hough transform and Gaussian filtering

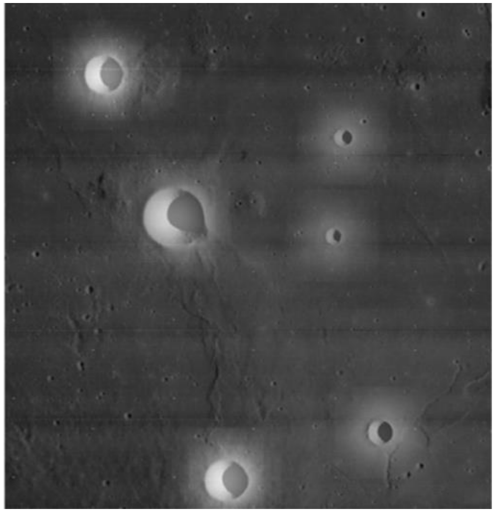

## Death Step

For **each ellipse** $\boldsymbol{x}_i$ in the configuration, compute the **death probability** as $d(\boldsymbol{x}_i)$:

$$d(\boldsymbol{x}_i) = \frac{\delta \cdot a(\boldsymbol{x}_i)}{1 + \delta \cdot a(\boldsymbol{x}_i)}$$

$$a(\boldsymbol{x}_i) = \exp\left[-\beta\left(U_L(X\backslash\{\boldsymbol{x}_i\}|C) - U_L(X|C)\right)\right]$$

# Crater Detection – Region Based Approach

**Region-Based Approach** → Why? →

- MBD is **computationally heavy**
- Computational burden increases with **image size**

## Region Based Flowchart and Example

Initialization
↓
Detection of **regions on interest** based on the birth map
↓
MBD in each **region**
↓
**Aggregation**

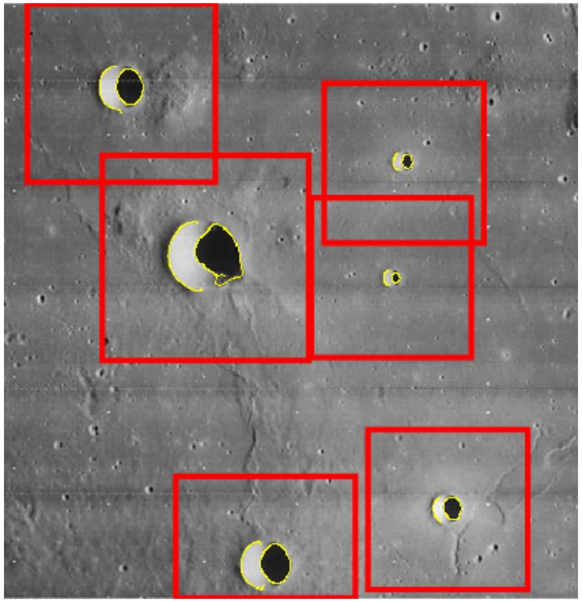

# Crater Detection – Data Sets

- 6 THEMIS (Thermal Emission Imaging System) images, TIR, 100m resolution, Mars Odissey mission
- 7 HRSC (High Resolution Stereo Color) images, VIS, ~20m resolution, Mars Express mission
- Image sizes from 1581 × 1827 to 2950 × 5742 pixels

**Quantitative Performance Assessment of the crater detection algorithm: Detection Percentage ($D$), Branching Factor ($B$), and Quality Percentage ($Q$)**

| Data | $D = \frac{TP}{TP + FN}$ | $B = \frac{FP}{TP}$ | $Q = \frac{TP}{TP + FP + FN}$ |
|---|---|---|---|
| Avg on all THEMIS | 0.91 | 0.10 | 0.83 |
| Avg on all HRSC | 0.89 | 0.06 | 0.85 |
| Avg on all images | 0.90 | 0.09 | 0.84 |

# Crater Detection – Results

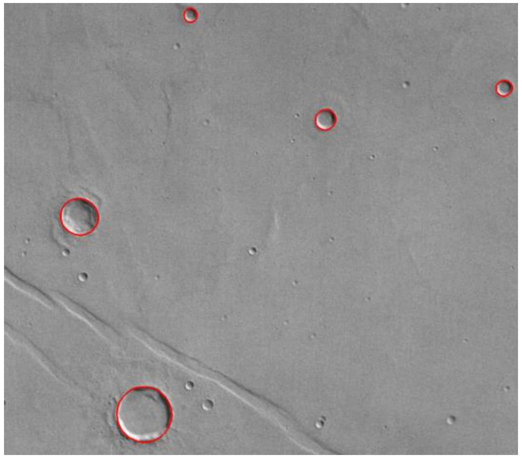

HRSC Sensor

| Crater | $C = (x_0, y_0)$ | Semi-axes $(a, b)$ | Orientation $\theta$ |
|---|---|---|---|
| Crater 1 | $(139, 393)$ | $(35, 33)$ | $64°$ |
| Crater 2 | $(258, 756)$ | $(51, 50)$ | $115°$ |
| Crater 3 | $(343, 23)$ | $(13, 12)$ | $180°$ |
| Crater 4 | $(591, 215)$ | $(19, 18)$ | $31°$ |
| Crater 5 | $(919, 157)$ | $(15, 14)$ | $106°$ |

Crater geometric properties extracted by the proposed method

HRSC Sensor

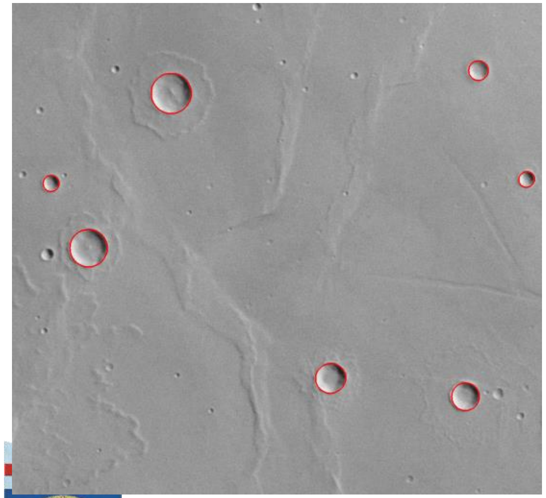

THEMIS Sensor

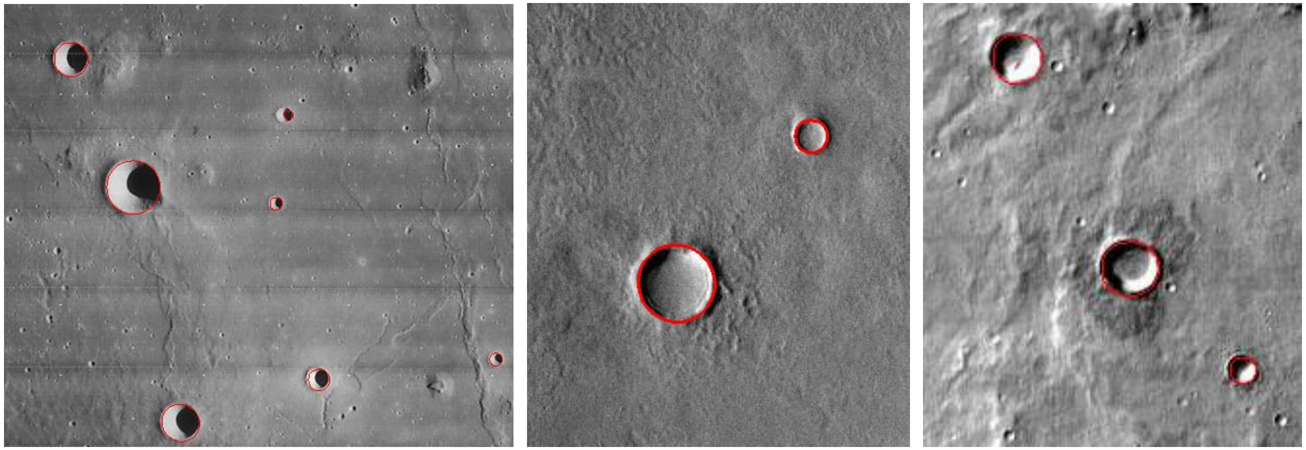

# Content

## Introduction

## Crater Detection

- Marked Point Process Model
- Energy Function
- Multiple Birth and Death Algorithm
- Region-of-Interest Approach
- Experimental Results

## Image Registration

- 2-step Approach
- Experimental Results

## Conclusion

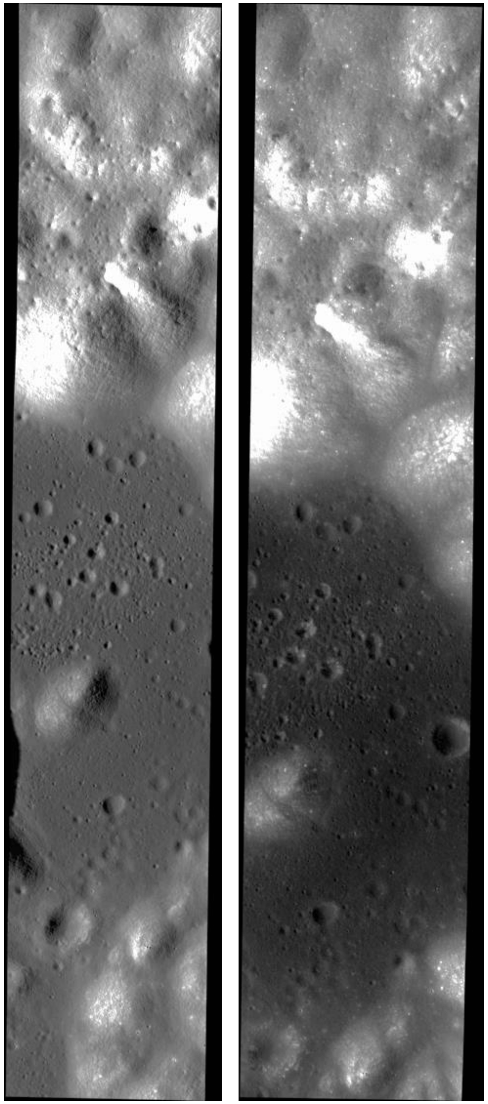

# Image Registration – 2-Step Optimization

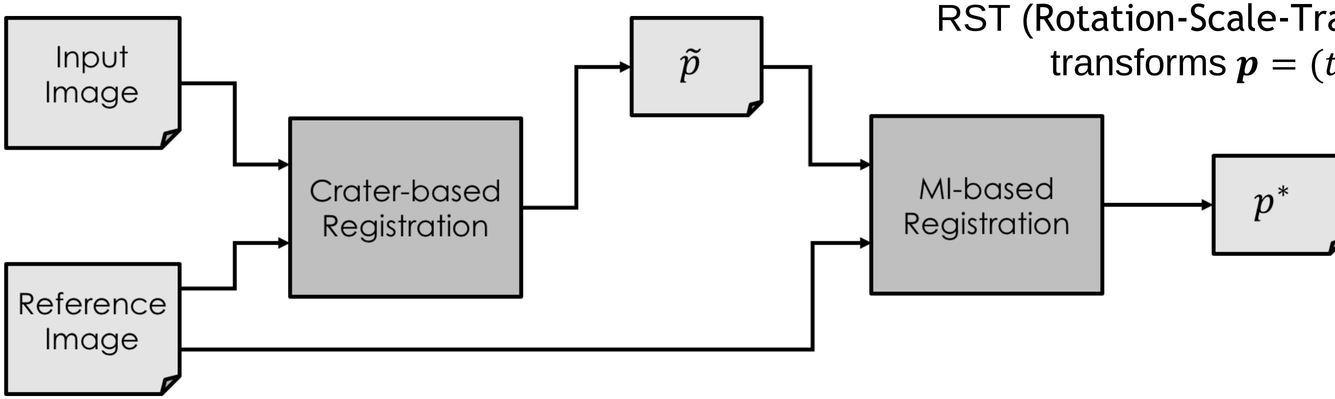


RST (Rotation-Scale-Translation)
transforms $\boldsymbol{p} = (t_x, t_y, \theta, k)$

## Why a 2-step Optimization?

**Feature-based registration**

- Min Hausdorff distance ($d_{\mathcal{H}}$) between extracted craters through genetic algorithm
- Fast but sensitive to accuracy of crater maps

**Area-based registration**

- Max Mutual Information ($MI$) through genetic algorithm
- Highly accurate but computationally heavy

Initialization

↓

**Fast registration** based on **extracted craters** → $\widetilde{\boldsymbol{p}}$

↓

**Refinement**: registration based on **mutual information** in a **neighborhood** of $\widetilde{\boldsymbol{p}}$ → $\boldsymbol{p}^*$

# Image Registration – Region of Interest

Transformation found for an interactively selected region of interest → $p_B^*$
$p_B = (t_x, t_y, \theta, k)$

Transformation derived for the entire Image → $p_A^*$
$p_A = (T_x, T_y, \beta, \alpha)$

$$p_A^* = \begin{pmatrix} -k\cos(\theta)\ x_0 - k\sin(\theta)\ y_0 + t_x + x_0 \\ k\sin(\theta)\ x_0 - k\cos(\theta)\ y_0 + t_y + y_0 \\ \theta \\ k \end{pmatrix}$$

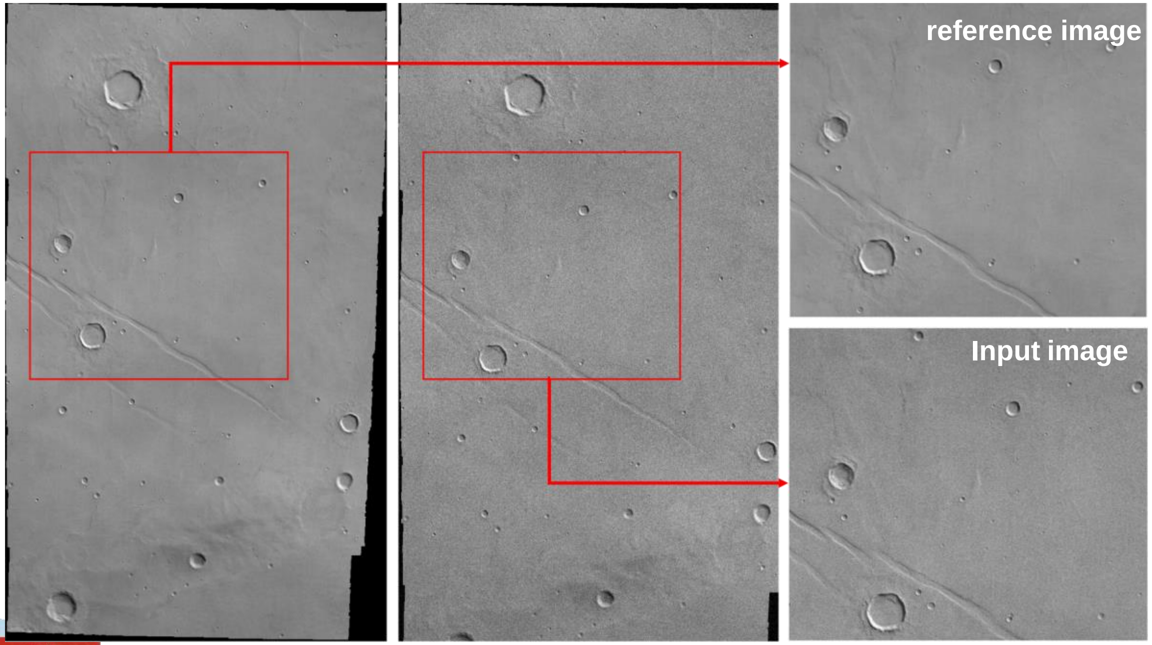


*Superposition of Reference and Input*

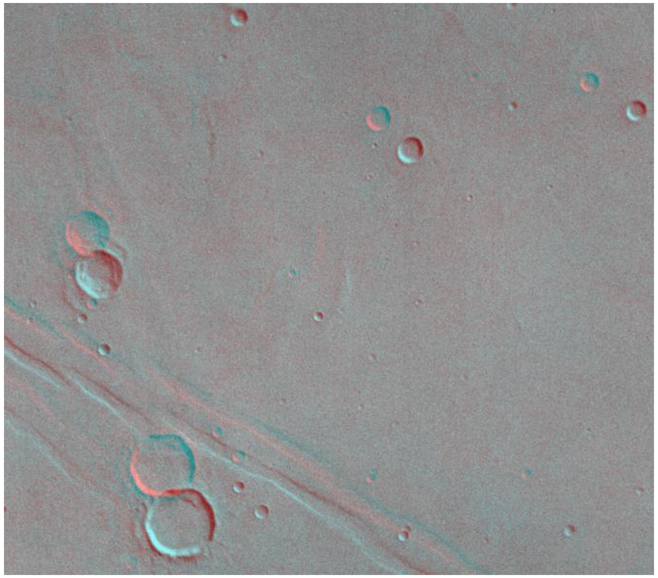

# Image Registration – Data Sets

**Semi-simulated image pairs**

20 pairs composed of one real THEMIS or HRSC image and of an image obtained by applying a synthetic transform and AWGN

*Quantitative validation with respect to the true transform (RMSE)*

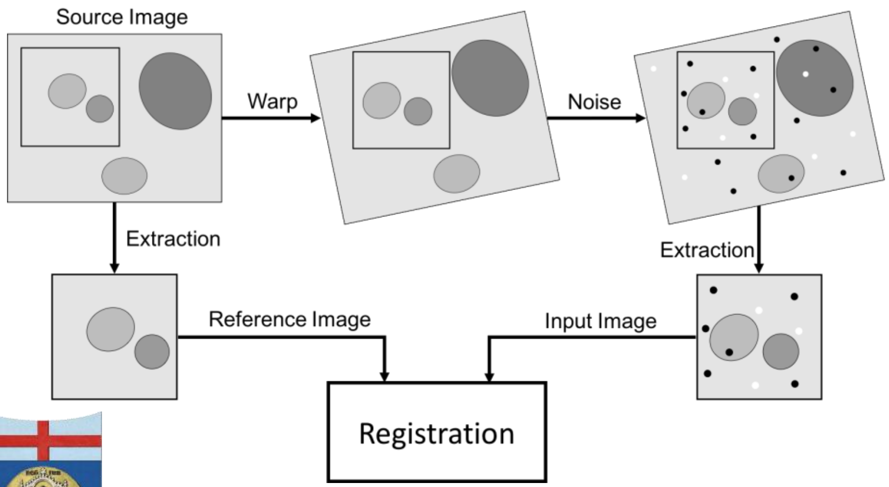


**Real multi-temporal image pairs**

Real multi-temporal pair of LROC (Lunar Reconnaissance Orbiter Camera) images

100m resolution

*Only qualitative visual analysis is available, as no ground truth is available*

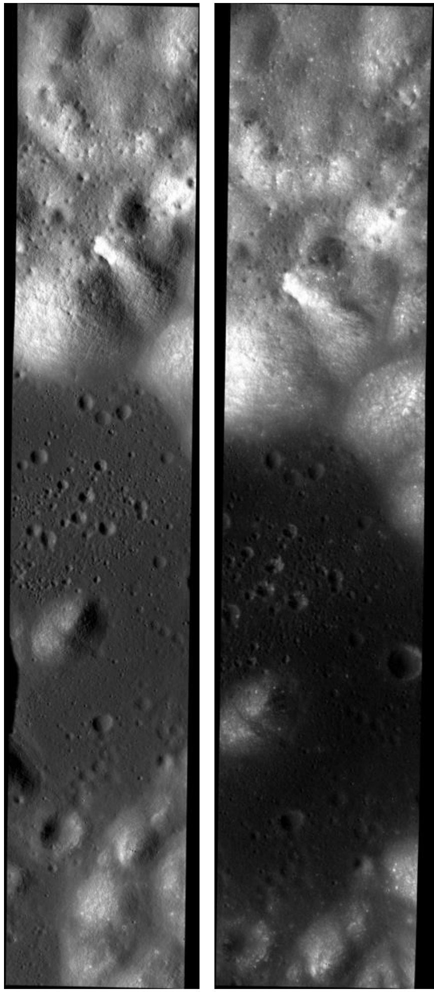

# Registration Results with Semi-synthetic Data

RGB of original non-registered data

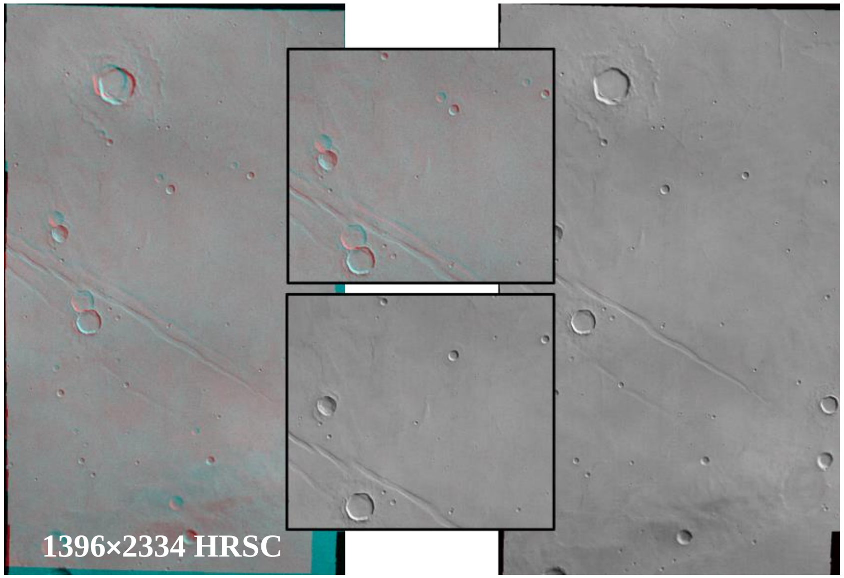


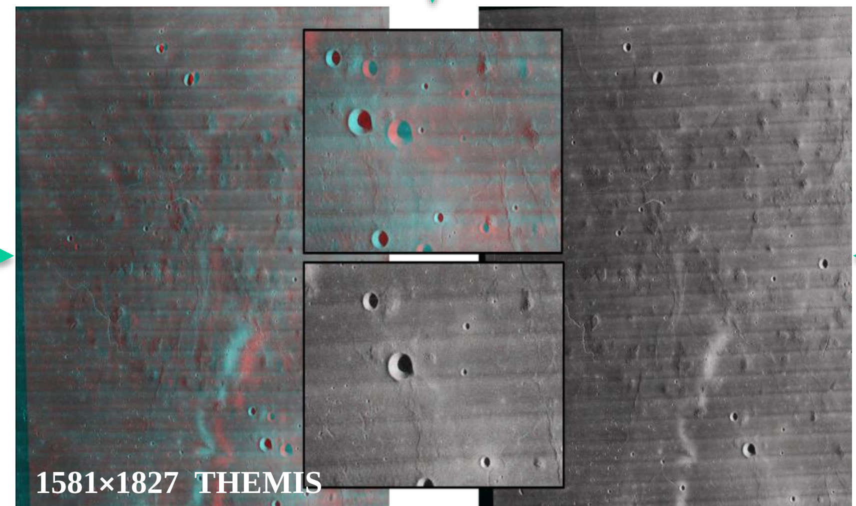


RGB of registered data

| Data set | RMSE [pixel] |
|---|---|
| THEMIS (10 data sets) | 0.31 |
| HRSC (10 data sets) | 0.22 |
| Average (20 data sets) | 0.26 |

| | Left Image | Right Image |
|---|---|---|
| $p_{GT}$ | $(7.05, 35.91, 0.18°, 1.071)$ | $(76.59, 19.96, 2.17°, 1.031)$ |
| $p^*$ | $(7.04, 35.92, 0.19°, 1.071)$ | $(76.41, 20.06, 2.18°, 1.031)$ |
| RMSE 1st Step | 0.79 | 0.51 |
| RMSE 2nd Step | 0.16 | 0.33 |

# Registration Results with Real Data

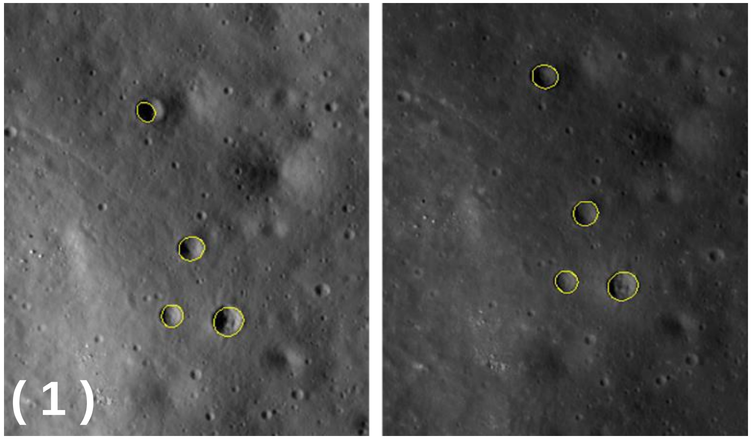


Visually accurate matching between reference and registered images in the real multitemporal data set

Checkerboard representation of the registered images (zoom on details)

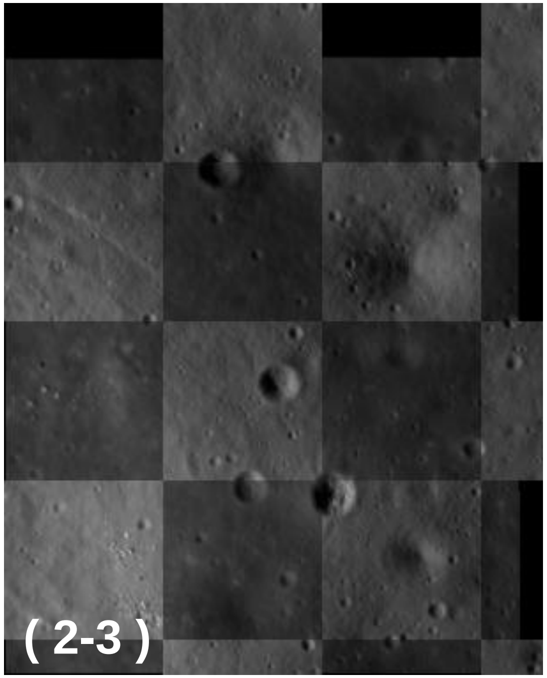


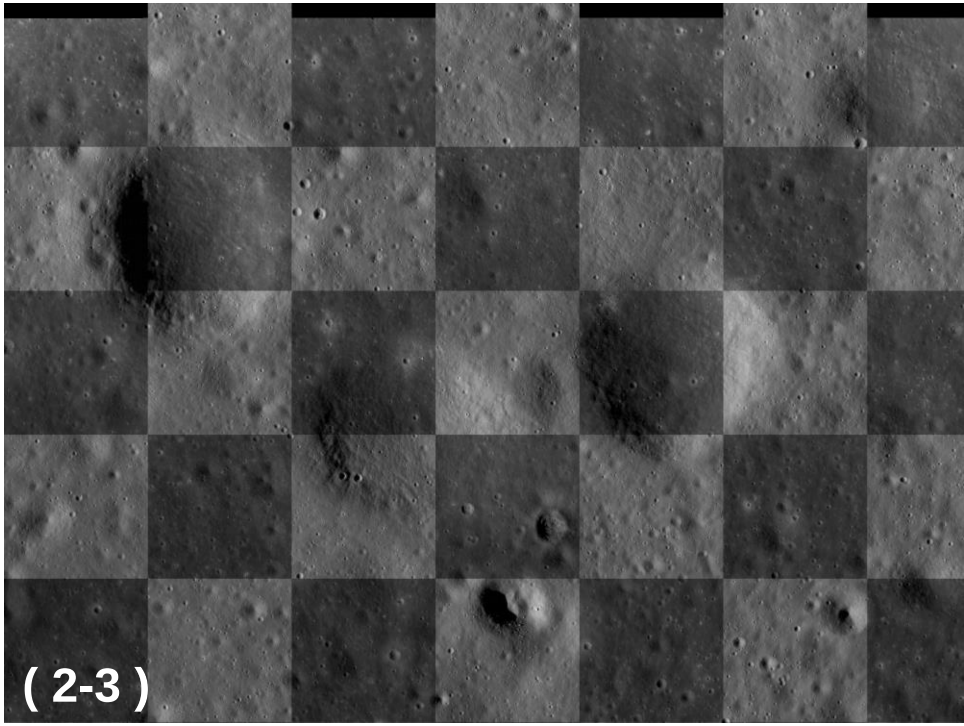

# Registration Results with Real Data

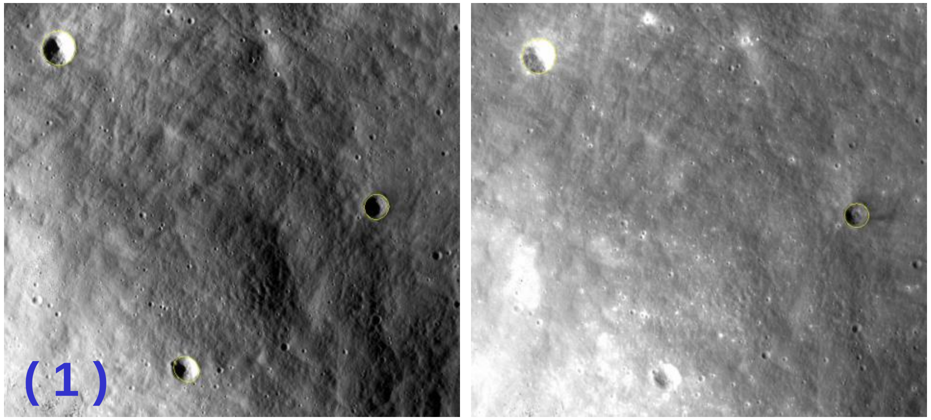


Visually accurate matching between reference and registered images in the real multitemporal data set

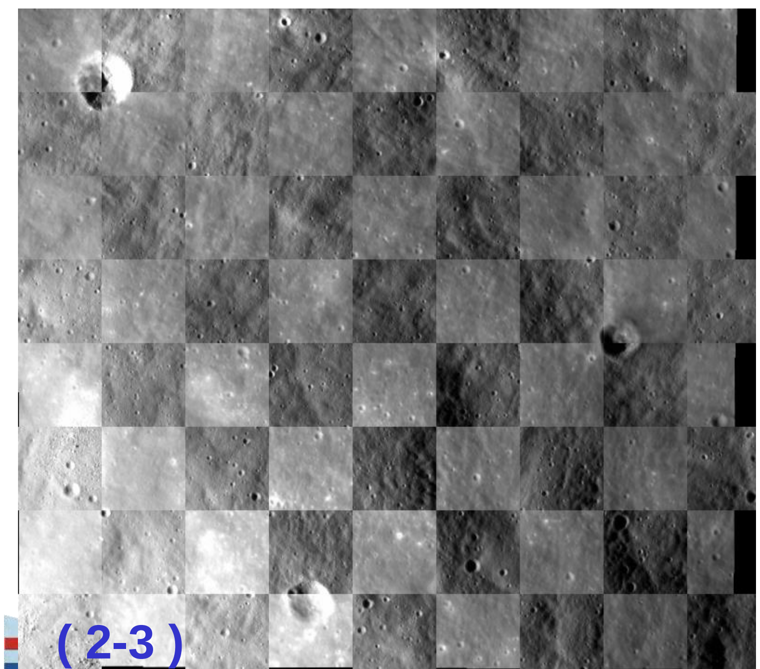


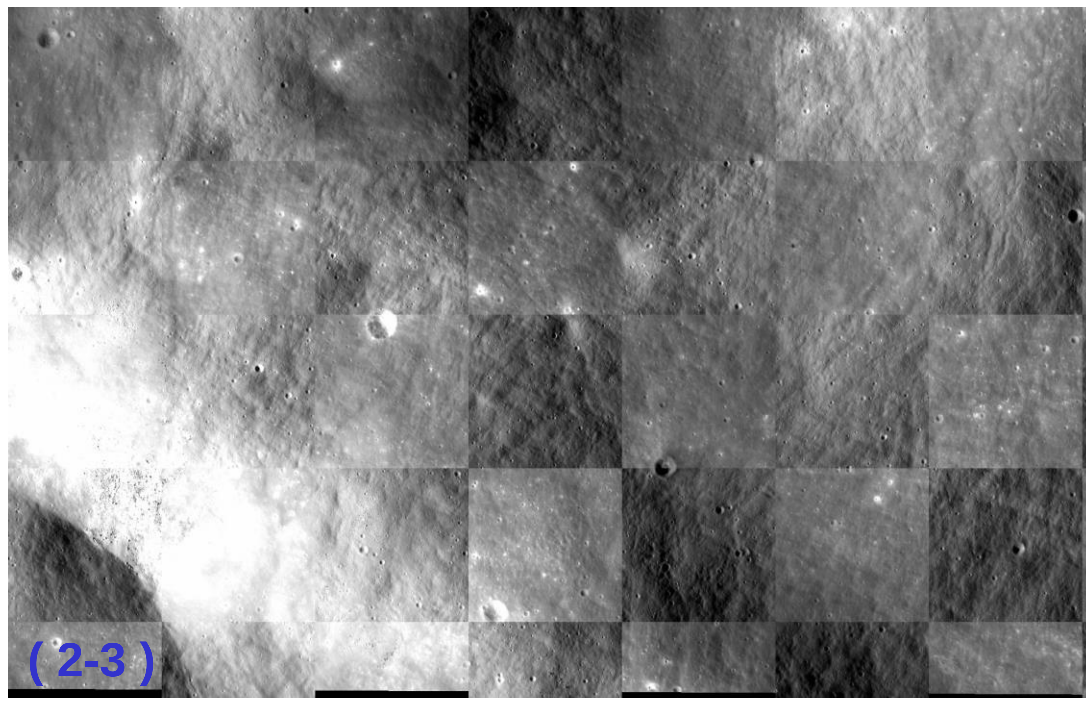

# Content

## Introduction

## Crater Detection

– Marked Point Process Model
– Energy Function
– Multiple Birth and Death Algorithm
– Region-of-Interest Approach
– Experimental Results

## Image Registration

– 2-step Approach
– Experimental Results

## **Conclusion**

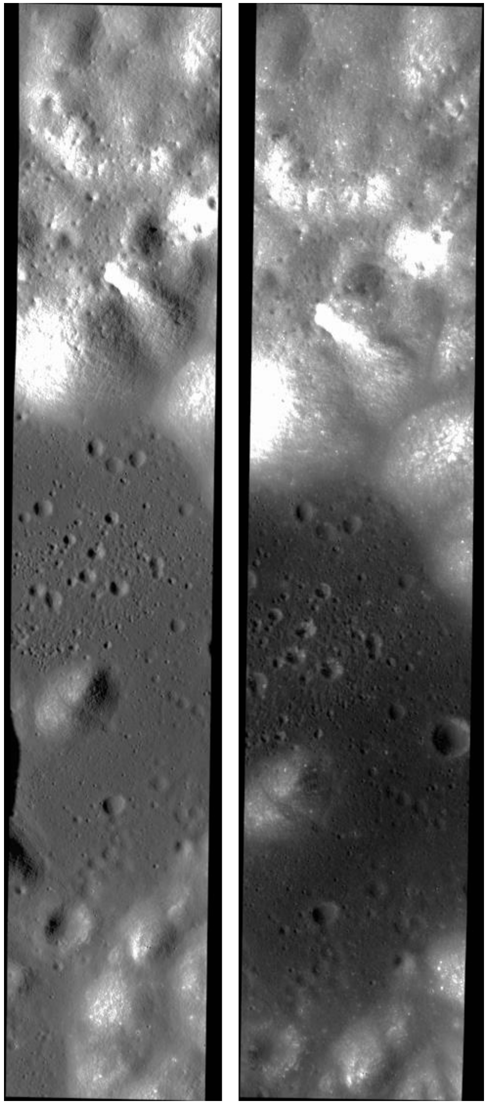

# Conclusions and Future Developments

## Conclusions

- **Accurate** crater maps, useful for both image registration and planetary science, were obtained from data from different sensors.
- **Higher accuracy** as compared to previous work on crater detection (not shown for brevity)
- Reduced time for convergence thanks to a **region-based approach**
- **Sub-pixel accuracy and visual precision** in registration: effectiveness of the proposed 2-step registration method

## Future Developments

- Test in conjunction with a **parallel** implementation (e.g. computer cluster)
- Validation with **multi-sensor** real images
- Extension to **other applications** requiring the extraction of ellipsoidal or circular features, e.g. optical Earth observation images or medical images

# Short Bibliography


- G. Troglio, J. A. Benediktsson, G. Moser and S. B. Serpico, "Crater Detection Based on Marked Point Processes," in *Signal and Image Processing for Remote Sensing*, CRC Press, 2012, p. 325–338.
- G. Troglio, J. Le Moigne, J. A. Benediktsson and G. S. S. B. Moser, "Automatic Extraction of Ellipsoidal Features for Planetary Image Registration," *IEEE Geoscience and Remote Sensing Letters,* vol. 9, pp. 95-99, 2012.
- S. Descamps, X. Descombes, A. Bechet and J. Zerubia, "Automatic Flamingo detection using a multiple birth and death process," in *IEEE International Conference on Acoustics, Speech and Signal Processing*, Las Vegas, NV, 2008.
- X. Descombes, R. Minlos and E. J. Zhizhina, "Object Extraction Using a Stochastic Birth-and-Death Dynamics in Continuum," *Journal of Mathematical Imaging and Vision,* vol. 33, p. 347–359, 2009.
- E. Zhizhina and X. Descombes, "Double Annealing Regimes in the Multiple Birth-and-Death Stochastic Algorithms," *Markov Processes and Related Fields, Polymath,* vol. 18, pp. 441-456, 2012.
- J. Le Moigne, N. S. Netanyahu and R. D. Eastman, Image Registration for Remote Sensing, Cambridge University Press, 2011.
- I. Zavorin and J. Le Moigne, "Use of multiresolution wavelet feature pyramids for automatic registration of multisensor imagery," *IEEE Transactions on Image Processing,* vol. 14, no. 6, pp. 770 - 782, 2005.
- J. M. Murphy, J. Le Moigne and D. J. Harding, "Automatic Image Registration of Multimodal Remotely Sensed Data With Global Shearlet Features," *IEEE Transactions on Geoscience and Remote Sensing,* vol. 54, no. 3, pp. 1685 - 1704, 2016.
- J. H. Holland, Adaptation in natural and artificial systems: an introductory analysis with applications to biology, control, and artificial intelligence, University of Michigan Press, 1975, p. 183.

# Appendix

# MBD – Birth Step

For **each pixel** in the image compute the **Birth Probability** as $\min\{\delta \cdot B(s), 1\}$, where:

$$B(s) = \frac{b(s)}{\sum_s b(s)}$$

Being $b(s)$ the **Birth Map** computed from the **Canny Contour Map**

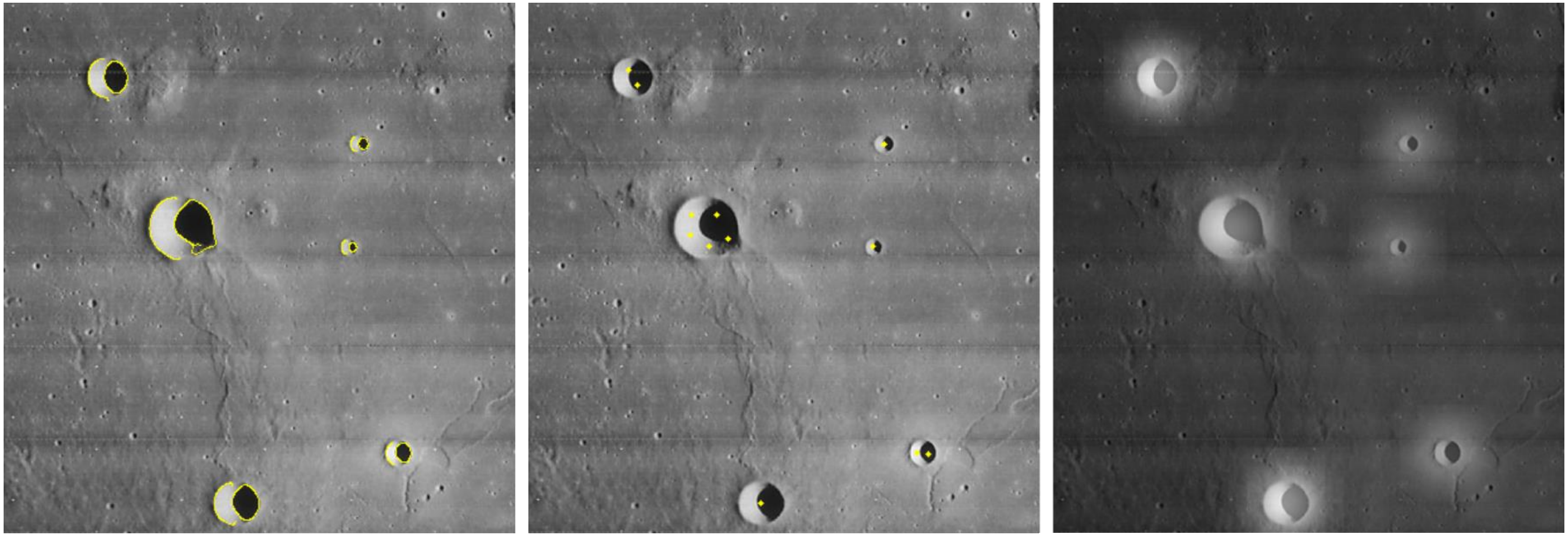

# MBD – Death Step

For **each ellipse** $x_i$ in the configuration compute the **Death Probability** as $d(x_i)$, where

$$d(x_i) = \frac{\delta \cdot a(x_i)}{1 + \delta \cdot a(x_i)} \quad \text{and} \quad a(x_i) = e^{-\beta\left(U_L(\{x \backslash x_i\}|I_g) - U_L(x|I_g)\right)} = e^{\beta \cdot U_L^i(x_i|I_g)}$$

The complete **Flowchart** of the **Death Step** is as follows:

Computation of the Energy Terms

↓

Computation of Death Prob. based on **Likelihood**

↓

Elimination of ellipses with prob. $d(x_i)$

↓

Configuration refinement thanks to **Prior** term

# Similarity Measures

## Hausdorff Distance

$$Similarity = mean_c \left\{ \sum_{i=1}^{N^c} \sum_{t=1}^{P} \left[ d_H\left(\underline{x}_i^c, \underline{x}_t\right) \right] \right\}$$

$\mathrm{c}$ = craters in Input Image
$\mathrm{N^c}$ = sum(pixels in crater c in Input Image)
$\mathrm{P}$ = sum(craters' border pixels in Ref Image)
$\underline{\mathrm{x}}_\mathrm{i}^\mathrm{c}$ = coord of pixel i in crater c in Input Image
$\underline{\mathrm{x}}_\mathrm{t}$ = coord of pixel t in Ref Image's craters

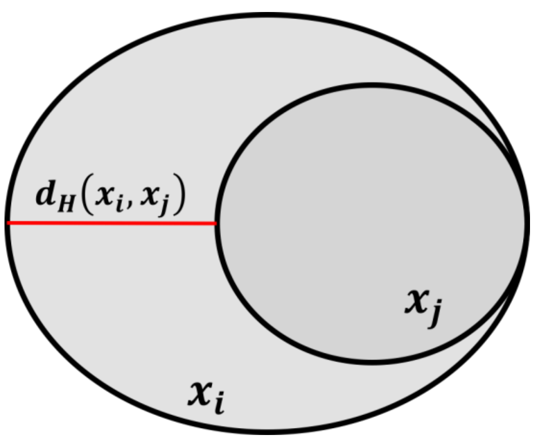


## Mutual Information

$$MI(X,Y) = \sum_{x \in X} \sum_{y \in Y} p_{X,Y}(x,y) \log \left( \frac{p_{X,Y}(x,y)}{p_X(x)\, p_Y(y)} \right)$$

$X$: pixel intensity in Reference Image
$Y$: pixel intensity in Input Image
$p_X(x)$: probability density function (pdf) of $X$
$p_Y(y)$: probability density function (pdf) of $Y$
$p_{X,Y}(x,y)$: joint pdf of $X$ and $Y$

$p_X(x)$ $\quad$ $p_Y(y)$ $\quad$ $p_{X,Y}(x,y)$

estimated through the corresponding image histograms

# RST Transformation

## Rotation – Scale – Translation Transformation

Transformation vector

$$p = (t_x, t_y, \theta, k)$$

$\{t_x, t_y\}$: Translations in $x$ and $y$

$\theta$: Rotation angle

$k$: Scaling Factor

Matrix Formulation

$$T_p(x,y) = \begin{pmatrix} k\cos(\theta) & k\sin(\theta) & t_x \\ -k\sin(\theta) & k\cos(\theta) & t_y \end{pmatrix} \begin{bmatrix} x \\ y \\ 1 \end{bmatrix}$$

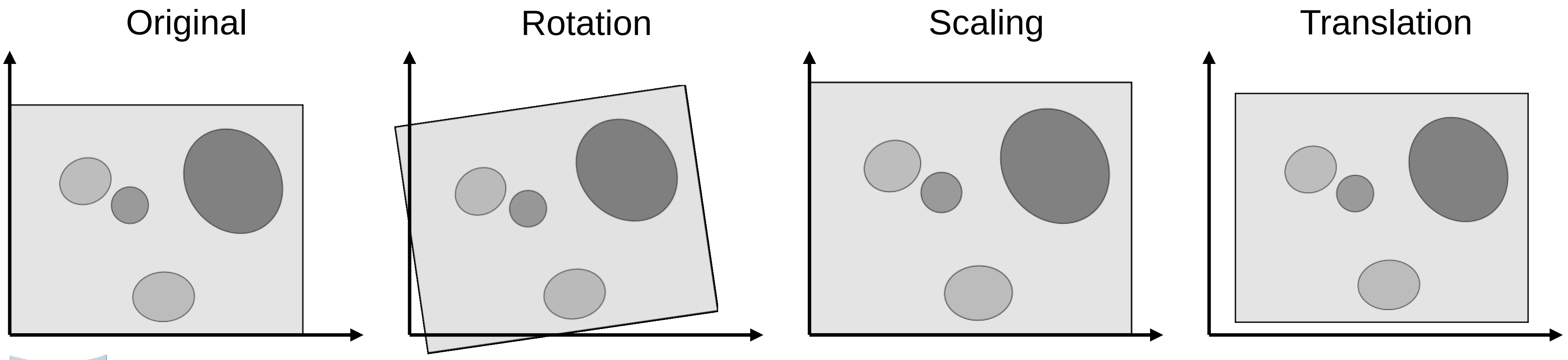

# Region of Interest Approach

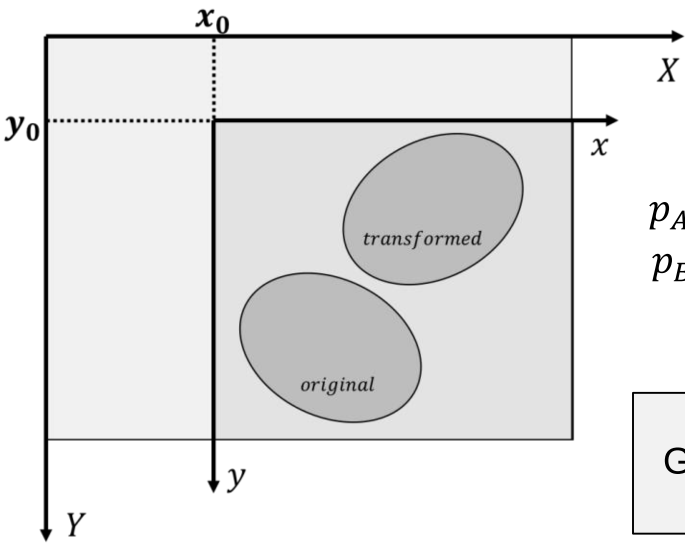


$I_A(X,Y), I_B(x,y)$: Two Images
$I_B$: sub-image of $I_A$ such that $I_B(0,0) = I_A(x_0,y_0)$

$p_A = (T_x, T_y, \beta, \alpha)$: RST transformation vector transforming $I_A$ into $I_A^{tr}$
$p_B = (t_x, t_y, \theta, k)$: RST transformation vector transforming $I_B$ into $I_B^{tr}$

$$I_B^{tr}(0,0) = I_A^{tr}(x_0,y_0)$$

Given: $\begin{cases} Transformation\text{: } p_B \\ Reference\ of\ Region\text{: } (x_0,y_0) \end{cases}$ → Find: $Transformation\text{: } p_A$

From the image

$$\begin{cases} X = x + x_0 \\ Y = y + y_0 \end{cases}$$

Expressing the transformation in Matrix Form

$$T_{p_A} = \begin{pmatrix} \alpha\cos(\beta) & \alpha\sin(\beta) & T_x \\ -\alpha\sin(\beta) & \alpha\cos(\beta) & T_y \end{pmatrix} \quad : \quad T_{p_A}(X,Y) = (X',Y')$$

$$T_{p_B} = \begin{pmatrix} k\cos(\theta) & k\sin(\theta) & t_x \\ -k\sin(\theta) & k\cos(\theta) & t_y \end{pmatrix} \quad : \quad T_{p_B}(x,y) = (x',y')$$

This should also hold

$$T_{p_A}(x+x_0, y+y_0) = (x'+x_0, y'+y_0)$$

Plugging $T_{p_A}$ into this equation and replacing $x'$ and $y'$ according to $T_{p_B}$

$$\begin{cases} k\cos(\theta)\,x + k\sin(\theta)\,y + t_x + x_0 = \\ \alpha\cos(\beta)(x+x_0) + \alpha\sin(\beta)(y+y_0) + T_x \\ \\ -k\sin(\theta)\,x + k\cos(\theta)\,y + t_y + y_0 = \\ -\alpha\sin(\beta)(x+x_0) + \alpha\cos(\beta)(y+y_0) + T_y \end{cases}$$

Knowing $\alpha = k$ and solving in $P_1 = (0,0)$ and $P_2 = (-x_0, -y_0)$

$$p_A = \begin{pmatrix} -k\cos(\theta)\,x_0 - k\sin(\theta)\,y_0 + t_x + x_0 \\ k\sin(\theta)\,x_0 - k\cos(\theta)\,y_0 + t_y + y_0 \\ \theta \\ k \end{pmatrix}$$

# RMS Error Computation

Ground Truth Transformation

$$p_{GT} = \left(t_{x1}, t_{y1}, \theta_1, k_1\right) \rightarrow T_{p_{GT}}(x,y) = Q_{p_{GT}} \cdot [x,y,1]^T$$

ComputedTransformation

$$p = \left(t_x, t_y, \theta, k\right) \rightarrow T_p(x,y) = Q_p \cdot [x,y,1]^T$$

Erorr Transformation

$$p_e = \left(t_{xe}, t_{ye}, \theta_e, k_e\right) \rightarrow Q_{P_e} = Q_p \cdot Q_{p_{GT}}^{-1}$$

$$\begin{cases} k_e = \dfrac{k_2}{k_1}, \qquad \theta_e = \theta_2 - \theta_1 \\ t_{xe} = t_{x2} - k_e\left(t_{x1}\cos(\theta_e) + t_{y1}\sin(\theta_e)\right) \\ t_{ye} = t_{y2} - k_e\left(t_{y1}\cos(\theta_e) - t_{x1}\sin(\theta_e)\right) \end{cases}$$

$(x,y) \in$ Image, $[x',y',1]^T = Q_{P_e} \cdot [x,y,1]^T$

$$\begin{bmatrix} x' \\ y' \end{bmatrix} = k_e \begin{pmatrix} \cos(\theta_e) & \sin(\theta_e) \\ -\sin(\theta_e) & \cos(\theta_e) \end{pmatrix} \begin{bmatrix} x \\ y \end{bmatrix} + \begin{bmatrix} t_{xe} \\ t_{ye} \end{bmatrix}$$

RMS Error: $E(p_e) = \sqrt{\frac{1}{AB}\int_0^A \int_0^B (x'-x)^2 + (y'-y)^2 dxdy}$, $\qquad \alpha = A^2 + B^2$

$$E^2(p_e) = \frac{1}{AB}\int_0^A \int_0^B (k_e\cos(\theta_e)\,x + k_e\sin(\theta_e)\,y + t_{xe} - x)^2 + \left(-k_e\sin(\theta_e)\,x + k_e\cos(\theta_e)\,y + t_{ye} - y\right)^2 dxdy$$

$$E^2(p_e) = \frac{\alpha}{3}(k_e^2 - 2k_e\cos(\theta_e) + 1) + \left(t_{xe}^2 + t_{ye}^2\right) - \left(At_{xe}^2 + Bt_{ye}^2\right)(1 - k_e\cos(\theta_e)) - k_e\left(At_{ye} - Bt_{xe}\right)\sin(\theta_e)$$